RSC Advances

PAPER

View Article Online
View Journal | View Issue

Cite this: *RSC Adv.*, 2022, **12**, 33207

Synthesis of silver nanoclusters by irradiation reduction and detection of Cr^{3+} ions

Fei Han,[b] Jihao Li,[ac] Wenrui Wang,[b] Mouhua Wang[a] and Linfan Li *[ac]

Received 17th October 2022
Accepted 9th November 2022

DOI: 10.1039/d2ra06536c

rsc.li/rsc-advances

In our work, a simple and fast synthesis method is provided to synthesize silver nanoclusters (AgNCs). In this method, with using polyacrylic acid (PAA) as a template, the silver ions were reduced to silver nanoclusters by irradiation reduction at room temperature. The prepared silver nanoclusters (PAA–AgNCs) with average particle size of 1.98 ± 0.79 nm have a fluorescence property, and their physical and chemical properties can be controlled by absorbed dose, PAA/Ag^+ mole ratio and other factors. The fluorescence stability of the PAA–AgNCs is good, and it is unique in that the fluorescence emission of the s PAA–AgNCs depends on the excitation wavelength. In addition, based on the fluorescence quenching phenomenon of PAA–AgNCs in the presence of Cr^{3+} ion, we established a simple and efficient method for the detection of Cr^{3+} ion by using PAA–AgNCs as fluorescent probes.

1 Introduction

Recently, metal nanoclusters (MNCs), especially Au nanoclusters and Ag nanoclusters, have attracted great interest because of their superior biological, physical and chemical properties.[1] In general, metal nanoclusters consist of several to several hundred metal atoms, most of which are around 2–3 nm in size or less than 2 nm.[2] Therefore, it is very important that metal nanoclusters provide a bridge between atoms and nanoparticles. Because they are similar in size to the electron Fermi wavelength,[3] metal nanoclusters tend to have discrete energy levels, resulting in their photoluminescence ability.[2,4] In particular, silver nanoclusters have excellent fluorescence performance[5] and have been proven to be an excellent candidate in fluorescent sensing,[6,7] catalysis[8] and biological imaging.[9,10]

At present, a large number of synthesis methods of silver nanocluster have been developed, such as chemical reduction,[11] photoreduction,[12] ultrasonic reduction,[13] *etc.* Although they are widely used in the synthesis of silver nanoclusters,[14–16] they often have some limitations, such as complex follow-up processing, the need for sophisticated instruments, low yield and so on. Here, we present a simple, easily controlled irradiation reduction synthesis method of water-soluble silver nanoclusters. Compared with other methods, irradiation reduction has the advantages of uniform and pure products, simple and controllable synthesis process and high yield.[17] In irradiation reduction, the key to the reduction process lies in the generation of reducing substances in the irradiation process: water molecules are ionized and excited by high energy gamma rays. And then, a large number of highly active components are produced by gamma rays in the solution, include e_{aq}^-, $HO^\bullet$, $H^\bullet$ and so on.[17,18] Among them, reductive materials such as e_{aq}^- can reduce metal ions to form primary particles, which eventually grow into metal nanoclusters *in situ*.[17,19,20] During this process, due to the strong penetration of gamma rays, reducing materials can be produced continuously and uniformly in the solution. On the other hand, the reducing materials come from the interaction between water and gamma rays, so the prepared silver nanoclusters are pure in the system.[17,21] Therefore, irradiation reduction in the synthesis of metal nanoclusters shows excellent feasibility.

Here, we report a synthesize method of water-soluble silver nanoclusters (PAA–AgNCs) by irradiation reduction with using PAA as template. As a polyelectrolyte, PAA is an excellent template for the synthesis of silver nanoclusters due to the strong binding ability of the carboxylate groups in PAA to silver ions.[22] In our study, the synthetic process and the fluorescence properties of PAA–AgNCs were studied. In addition, we found that the fluorescence of prepared PAA–AgNCs were quenched in the presence of Cr^{3+} ions. Thus, in this study, we further established an efficient and fast method for the quantitative detection of Cr^{3+} ions by using prepared PAA–AgNCs as fluorescent probes.

2 Experimental

2.1 Chemicals and materials

Sodium polyacrylate (PAA) was purchased from Sigma-Aldrich (Shanghai, China). Silver nitrate ($AgNO_3$), isopropanol and chromium nitrate ($Cr(NO_3)_3$) were purchased from Sinopharm

[a]*Shanghai Institute of Applied Physics, Chinese Academy of Sciences, Shanghai 201800, China. E-mail: lilinfan@sinap.ac.cn*
[b]*University of Chinese Academy of Sciences, Beijing 100049, China*
[c]*Wuwei Institute of New Energy, Gansu, 733000, China*

Chemical Reagent Co., Ltd. (Shanghai, China). All chemicals and solvents were analytical reagent (AR) and employed as received without further purification. Milli-Q water was used for all experiments.

2.2 Apparatus

The detailed size of prepared silver nanoclusters were observed using high-resolution transmission electron microscopy (HR-TEM; JEM-3000F, JEOL, Ltd.). UV-vis spectra were obtained using a quartz cuvette with absorption wavelengths from 300 nm to 800 nm. Fluorescence intensity was recorded by a FS5 Fluorescence spectrophotometer with an excitation wave length of 517 nm, an excitation and emission slit width of 3/3 nm and a photomultiplier tube voltage of 400 V in emission mode.

2.3 Preparation of PAA–AgNCs

PAA–AgNCs were synthesized by irradiation reduction. First, sodium polyacrylate solution was prepared from sodium polyacrylate powder by 20 min ultrasonic dissolution in 16 mL deionized water. Then, the prepared sodium polyacrylate solution was added to the 4 mL fresh prepared silver nitrate solution drop by drop under agitation, and the mixed solution was stirred for 1 h to make the carboxylate in sodium polyacrylate fully combine with silver ions. Make sure that the concentration of sodium polyacrylate and silver nitrate in the mixture is 0.02 M. Then, 0.601 g isopropanol was added to the mixture as an oxidizing free radical scavenger with vigorous stirring for 1 h. The solution was sparged with N_2 for 15 min, and then radiated at appropriate absorbed dose through Co_{60}. The total synthesis process was conducted at room temperature. After irradiation, the solution changes from colorless to blue, the prepared PAA–AgNCs solution were stored in the refrigerator at 4 °C, hidden from light. In order to clearly and accurately describe the synthesis conditions of the sample, the sample synthesized at 600 Gy absorbed dose, 0.02 M silver nitrate concentration, 1/1 molar ratio of PAA to silver nitrate, and 0.5 M isopropanol concentration was named AgNCs-1. In the subsequent experimental exploration, the control variable method with only one variable changed was introduced into the study of the synthesis process of AgNCs.

2.4 Fluorescence detection of Cr^{3+} ions

A stock solution of Cr^{3+} ions was prepared by dissolving a certain amount of chromium nitrate solid in deionized water. The stock solution of Cr^{3+} ions was properly diluted into standard working solutions of different concentrations for further research by adding deionized water. Typically, 1 mL of standard working solutions of Cr^{3+} ions was added into 1 mL of PAA–AgNCs stock solution. Then, the mixture oscillates for 2 hours before fluorescence measurements.

2.5 UV-visible spectroscopy

3 mL prepared silver nanoclusters solution was transferred into a quartz cuvette, and then the cuvette was transferred into an ultraviolet spectrophotometer with water as the background reference for measurement.

2.6 Fluorescence spectroscopy

400 μL prepared silver nanoclusters solution was transferred into a fluorescent quartz cuvette through a pipette, and then the fluorescent quartz cuvette was transferred into a fluorescence spectrophotometer for measurement.

3 Results and discussion

3.1 Synthesis of AgNCs

In this work, using PAA as template and isopropanol as oxidative free radical scavenger, silver nanoclusters (PAA–AgNCs) were prepared by gamma ray (Scheme 1), and the silver nanoclusters obtained had smaller particle size and photoluminescence ability. As shown in Fig. 1a, after irradiation, the initially colorless solution gradually turns blue, it has obvious characteristic absorption peaks at 500 nm and 700 nm. Meanwhile, the PAA–AgNCs produced red fluorescence emission at 679 nm upon excitation at 517 nm (Fig. 1b). Fig. 1c shows the TEM image of the prepared PAA–AgNCs. As shown in the Fig. 1c, the prepared silver nanoclusters are all spherical and wrapped in PAA, with an average particle size of 1.98 ± 0.79 nm. This is consistent with other work.[23] To investigate the synthesis process of the PAA–AgNCs, we investigated the effects of a series of related parameters on the synthesis process, including absorbed dose, isopropanol content, PAA/Ag^+ mole ratio and concentration.

3.1.1 Absorbed dose. The changes in the properties of PAA–AgNCs prepared with different absorbed dose has proved interesting. Fig. 1 shows the changes of ultraviolet absorption, fluorescence emission and morphology of PAA–AgNCs at different absorption dose. The samples described in the figure were prepared with different absorbed dose on the basis of AgNCs-1 only by changing the absorbed dose. Before irradiation, the mixed solution showed no absorption in the range of 400–800 nm (Fig. 1a). As shown in Fig. 1a, when the absorption dose reached 600 Gy, the absorption peak at 500 nm and 700 nm appeared respectively. As the absorption dose increasing, the absorption peak at 500 nm was weakened, but the absorption peak at 700 nm continued to increase. When the absorbed dose reached 500 Gy, the absorption peak of 500 nm almost disappeared, and the absorption peak of 700 nm was enhanced with a certain red shift. Fig. 1b shows that the fluorescence intensity of PAA–AgNCs increases first and then decreases with the increase of absorbed dose. Before irradiation, the solution of the system did not show fluorescence under 517 nm light excitation. Then, after irradiation, the prepared PAA–AgNCs solution showed fluorescence emission of 679 nm under excitation. When the absorbed dose reaches the higher dose, fluorescence emission of PAA–AgNCs gradually weakened, which is similar to the change of absorption at 500 nm of UV-vis spectra (Fig. 1a and b). The consistent change between fluorescence emission and absorption peak at 500 nm indicates that the characteristic absorption peak at 500 nm is generated by the

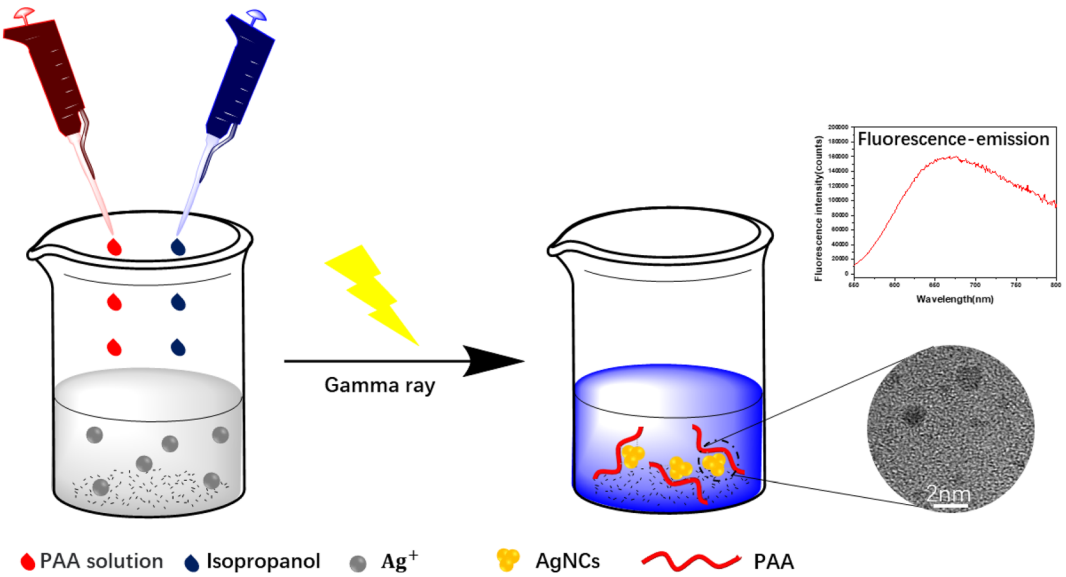

Scheme 1 Synthetic process of AgNCs.

PAA–AgNCs with fluorescence emission. Similar results have been reported previously, in which silver nanoclusters were synthesized by using PMAA as a template.[12,13,24] In addition, TEM images (Fig. 1c and d) also showed that at higher absorbed dose, the particle size of the prepared nanoclusters was slightly higher than that of silver nanoclusters at lower absorbed dose, and obvious agglomeration phenomenon occurred to form large non-fluorescent nanoparticles. This indirectly proves that low absorbed dose is more conducive to the formation of nanoclusters.

3.1.2 Isopropanol concentration. During irradiation, water molecules under the action of gamma rays can produce both oxidized radicals and reduced radicals.[18] In general, to avoid the reaction of oxidized radicals with silver nanoclusters, it is necessary that oxidized radical scavengers are added to the synthesis system to inhibit this process.[18,19] In this study, the scavenging ability of isopropanol on oxidized radicals and the effect of its content on the synthesis process in silver nanocluster synthesis system were investigated. The samples described in the Fig. 2 were prepared with different absorbed dose on the basis of AgNCs-1 only by changing the isopropanol contents. As shown in Fig. 2a and b, after adding isopropanol, the absorption peak of PAA–AgNCs at 500 nm is more obvious, and the fluorescence intensity was also stronger than that of the

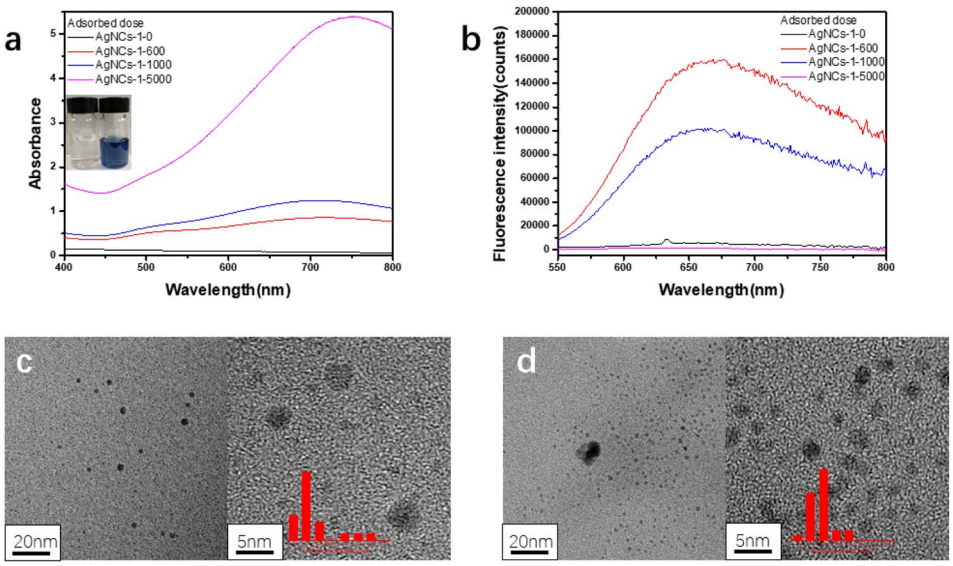

Fig. 1 (a) UV-vis spectra of silver nanoclusters at different absorption dose, inset: silver nanocluster solution before irradiation (left) and after irradiation (right); (b) fluorescence spectra of nanoclusters; (c) TEM image of silver nanocluster (AgNCs-1-600), inset: particle size distribution of AgNCs; (d) TEM image of silver nanocluster (AgNCs-1-1000), inset: particle size distribution of AgNCs; the samples were named as AgNCs-1-0, AgNCs-1-600, AgNCs-1-1000, AgNCs-1-5000, and their absorbed dose were 0 Gy, 600 Gy, 1000 Gy, and 5000 Gy, respectively.

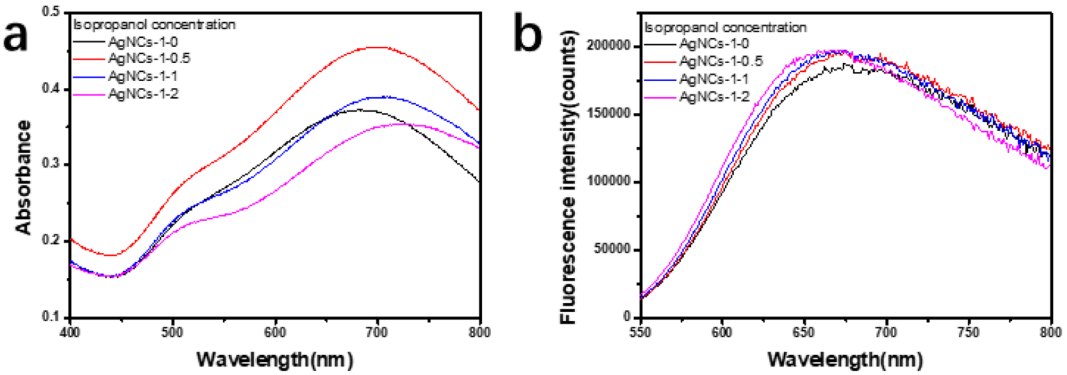

Fig. 2 UV-vis spectra (a) and fluorescence spectra (b) of PAA–AgNCs with different isopropanol contents; the samples were named as AgNCs-1-0, AgNCs-1-0.5, AgNCs-1-1, AgNCs-1-2, and their isopropanol contents were 0 M, 0.5 M, 1 M, and 2 M, respectively.

silver nanocluster solution without isopropanol. In addition, after adding 0.5 M isopropanol, even if the concentration of isopropanol was further increased, the fluorescence intensity of PAA–AgNCs was not further improved (Fig. 2b). This indicates that at the absorbed dose of 600 Gy, 0.5 M isopropanol is sufficient to maintain the reducing atmosphere of the system. And the fluorescence intensity of PAA–AgNCs is not affected even if there is excess isopropanol. Considering that the increase of fluorescence intensity of the PAA–AgNCs is limited after the addition of isopropanol, the synthesis system of AgNCs can be further simplified by not adding isopropanol, which is more conducive to the simple and rapid synthesis of AgNCs. However, in this work, in order to ensure that the synthesis process is always in a reducing atmosphere, 0.5 M isopropanol was used in the synthesis process of PAA–AgNCs.

3.1.3 PAA/Ag^+ mole ratio. During the synthesis process of PAA–AgNCs, the coordination interaction between silver ions and carboxylate groups in PAA is very important for the stability of silver nanoclusters.[12,25] Fig. 3 shows the UV-vis spectra and fluorescence spectra of PAA–AgNCs with different PAA/Ag^+ mole ratio at the 600 Gy absorbed dose. The samples described in the figure were prepared with different absorbed dose on the basis of AgNCs-1 only by changing the PAA/Ag^+ mole ratio at a constant PAA concentration of 0.02 M. The higher the relative concentration of carboxylate groups lead to higher absorption peak at 500 nm (Fig. 3a) and stronger fluorescence intensity (Fig. 3b). With the increase of silver ion concentration, the absorption peak of PAA–AgNCs at 500 nm gradually weakened (Fig. 3a), and the fluorescence intensity also decreased (Fig. 3b). This may be due to the tendency of silver nanoclusters to

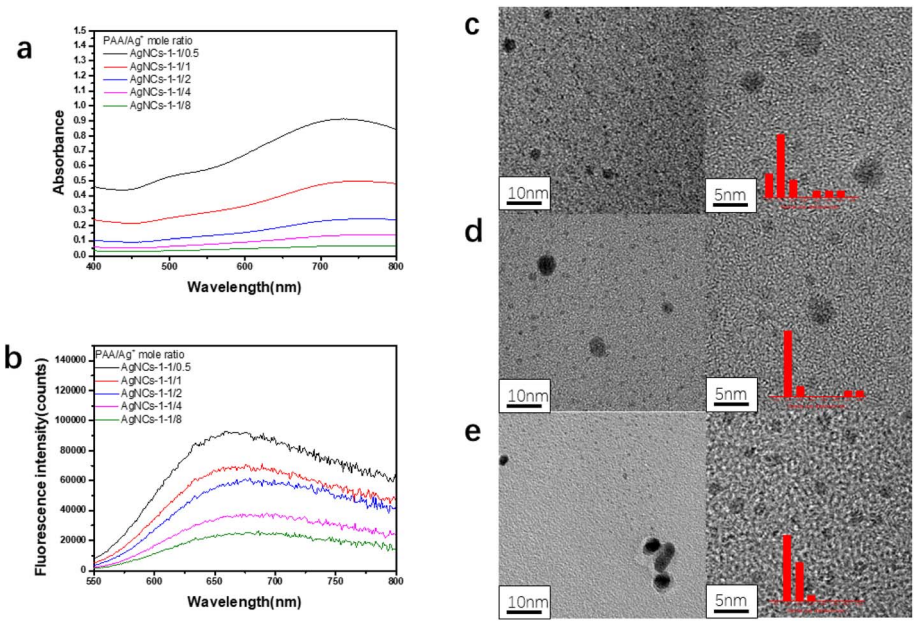

Fig. 3 UV-vis spectra (a) and fluorescence spectra (b) of PAA–AgNCs with different PAA/Ag^+ mole ratio; (c–e), TEM images of PAA–AgNCs with different PAA/Ag^+ mole ratio: (c) AgNCs-1-1/1; (d) AgNCs-1-1/4; (e) AgNCs-1-1/8; the samples were named as AgNCs-1-2/1, AgNCs-1-1/1, AgNCs-1-1/2, AgNCs-1-1/4, AgNCs-1-1/8, and their PAA/Ag^+ mole ratio were 2/1, 1/1, 1/2, 1/4 and 1/8, respectively.

aggregate and form larger nanoparticles at high silver ion concentration. When the relative concentration of PAA is high, the aggregation of PAA–AgNCs was weak (Fig. 3c). With the increase of the relative concentration of silver ions, large nanoparticles appear in TEM (Fig. 3d and e), showing a more obvious aggregation phenomenon. Large nanoparticles will be produced in PAA–AgNCs (Fig. 3c–e) at high silver ion concentration, which is not conducive to the formation of AgNCs (Fig. 3a) and leads to the decrease of fluorescence intensity of PAA–AgNCs (Fig. 3b). The formation of larger nanoparticles may be due to the fact that the limited carboxylate groups cannot stabilize the existence of all the silver nanoclusters in the case of high silver ion concentration, resulting in the spontaneous aggregation of silver nanoclusters into nanoparticles. Thus, the fluorescence intensity of PAA–AgNCs decreased at high silver ion concentration. As is shown above (Fig. 3d and e), with the improvement of silver ion concentration, although the nanoparticles gradually appeared in the PAA–AgNCs, but nanoclusters are still there. And under the different concentration of silver ion, the particle size of nanoclusters is relatively close to. This also proves that nanoparticles are formed by agglomeration of silver nanoclusters that are not stabilized by PAA, rather than by the silver nano clusters grow gradually formed. Based on the above rules, a higher relative molar concentration of PAA (PAA/Ag^+ molar ratio of 2/1) was used for the synthesis of silver nanoclusters, and AgNCs-1-2/1 was named as AgNCs-2.

3.1.4 System concentration. In addition, the effect of concentration on silver nanocluster synthesis was investigated. On the basis of AgNCs-2, the samples shown in the figure were prepared with different concentrations by maintaining a constant PAA/Ag^+ molar ratio (2/1) and only changing the concentration of silver nitrate. The Fig. 4a shows that the absorption of 500 nm increases gradually with the increase of system concentration. This indicates that higher concentrations of silver nanoclusters are produced. However, the fluorescence spectra (Fig. 4b) of PAA–AgNCs showed a trend of first rising and then decreasing with the increase of system concentration. This is due to the phenomenon of self-quenching of the high concentration of silver nanoclusters, which leads to the decrease of fluorescence intensity of the nanoclusters. This is consistent with previous other reports.[12,22]

3.2 Fluorescence of AgNCs

A unique feature of silver nanoclusters is fluorescence, which is not observed for Ag nanoparticles.[5] It can be seen from Fig. 1c that under the excitation at 517 nm, the silver nanocluster

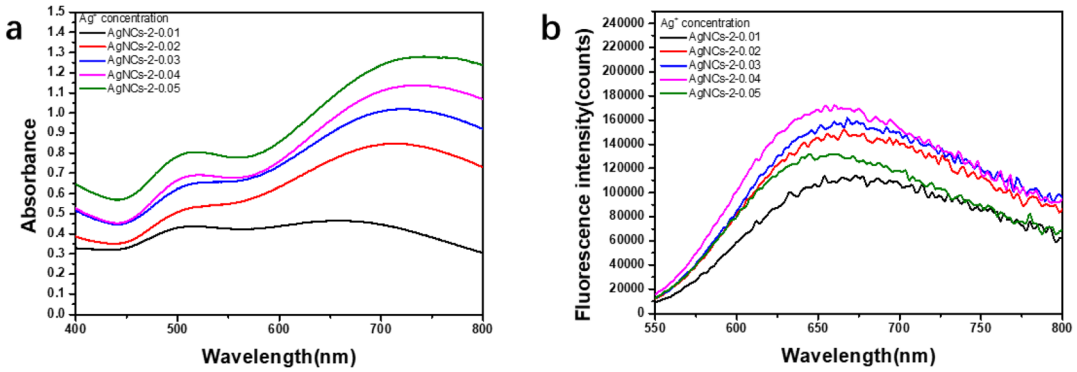

Fig. 4 UV-vis spectra (a) and fluorescence spectra (b) of PAA–AgNCs with different initial concentrations; the samples were named as AgNCs-2-0.01, AgNCs-2-0.02, AgNCs-2-0.03, AgNCs-2-0.04, AgNCs-2-0.05, and their silver nitrate concentrations were 0.01 M, 0.02 M, 0.03 M, 0.04 M and 0.05 M, respectively.

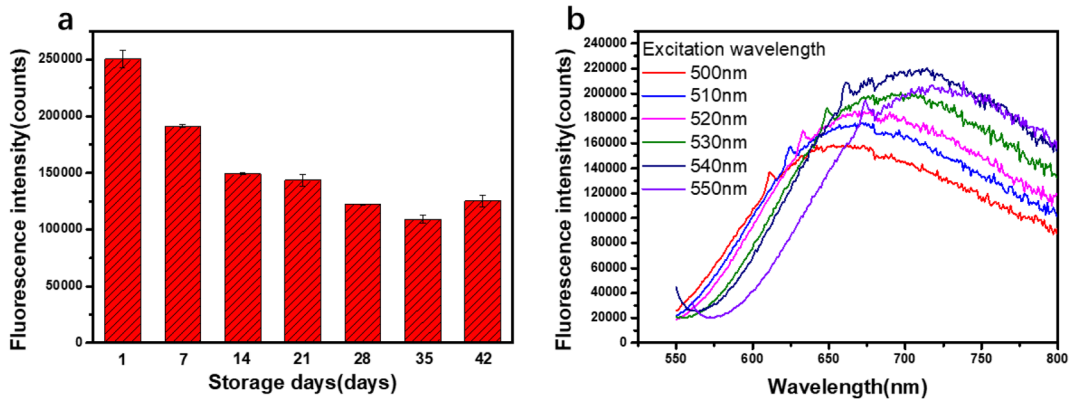

Fig. 5 (a) The fluorescence intensity of PAA–AgNCs with different number of storage days; (b) fluorescence spectra of PAA–AgNCs with different excitation wavelengths.

(AgNCs-2) produces a red fluorescence emission at 679 nm. The quantum yield is 0.19, calculated by use of rhodamine B in ethanol as a reference. Due to the small size of silver nanoclusters, silver nanoclusters tend to aggregate with each other to form non-fluorescent silver nanoparticles in order to reduce the surface energy, so fluorescence stability is one of the important properties of silver nanoclusters.[20] The Fig. 5a shows the fluorescence changes of the nanoclusters with the extension of the storage time. After 30 days of dark storage at 4 °C, the fluorescence intensity was only slightly lower than the initial fluorescence intensity, indicating that the prepared PAA–AgNCs had better fluorescence stability.

In addition, we found that the fluorescence emission of PAA–AgNCs is dependent on the excitation wavelength. As shown in the Fig. 5b, with the increase of the excitation wavelength, the fluorescence intensity of the silver nanocluster increases first and then decreases, and the maximum fluorescence emission peak appears red shift. This may indicate that the prepared PAA–AgNCs are composed of silver nanoclusters containing a different number of silver atoms. To date, all silver nanoclusters prepared by any synthetic method have generally exhibited this similar phenomenon.[4,22,26]

3.3 Detection of Cr^{3+} ions

Cr^{3+} ions can have a serious effect on cell structure by binding to DNA and can do great harm to the human body.[27] Meanwhile, it is widely used in agriculture and industry. So it is also an important environmental pollutant.[28] Therefore, it is very important to develop a quick and sensitive detection reduction method of Cr^{3+} ions. The prepared PAA–AgNCs (AgNCs-2) show obvious fluorescence quenching in the presence of Cr^{3+} ions (Fig. 6a), so the silver nanoclusters synthesized by irradiation method can be used for the detection of Cr^{3+} ions.

To confirm the feasibility of proposed detection strategy, we investigated the fluorescence intensity of prepared PAA–AgNCs in the presence of different concentrations of Cr^{3+} ions. The obtained fluorescence quenching data were analyzed by Stern–Volmer fluorescence quenching equation:[29]

$$\frac{F_0}{F} = K_{SV}C + 1$$

where F_0 is the fluorescence intensity of the control group without Cr^{3+} ions at 679 nm, F is the fluorescence intensity of PAA–AgNCs with different concentrations of Cr^{3+} ions at 679 nm, K_{SV} is Stern–Volmer fluorescence quenching constant, and C is Cr^{3+} ions concentration. The Fig. 6b shows the relationship between the fluorescence intensity of the silver nanocluster with different concentrations of Cr^{3+} ions and the concentration of Cr^{3+} ions. As shown in Fig. 6c, the fitted curve has a good linear relationship in range of 0.001 M to 0.01 M, the linear equation is $\frac{F_0}{F} = 116.44C + 1$, and the linear correlation coefficient is 0.99865. The detection limit was calculated, following the IUPAC criterion,[14] as the concentration of Cr^{3+} ions which produced an analytical signal three times the standard deviation of the blank signal. The result then suggested a detection limit as low as 0.000703 M. This fully proves that the prepared PAA–AgNCs can be used in detection of Cr^{3+} ions.

Generally, there are two mechanisms leading to fluorescence quenching of PAA–AgNCs, one is static quenching and the other is dynamic quenching.[6] In order to explore the mechanism of fluorescence quenching of PAA–AgNCs by Cr^{3+} ions, the above two quenching mechanisms were examined. The average FL lifetimes of the PAA–AgNCs (τ_0) and PAA–AgNCs with Cr^{3+} ions (τ) were estimated to be approximately 0.74 ns and 0.62 ns, respectively. The fluorescence lifetime of PAA–AgNCs before and after exposure to Cr^{3+} ions has only a small change, thus the fluorescence quenching mechanism is more inclined to static quenching.[6] It is well known that PAA is a polyelectrolyte, and the carboxylic acid on the molecular chain has coordination effect with many metal ions, and Cr^{3+}

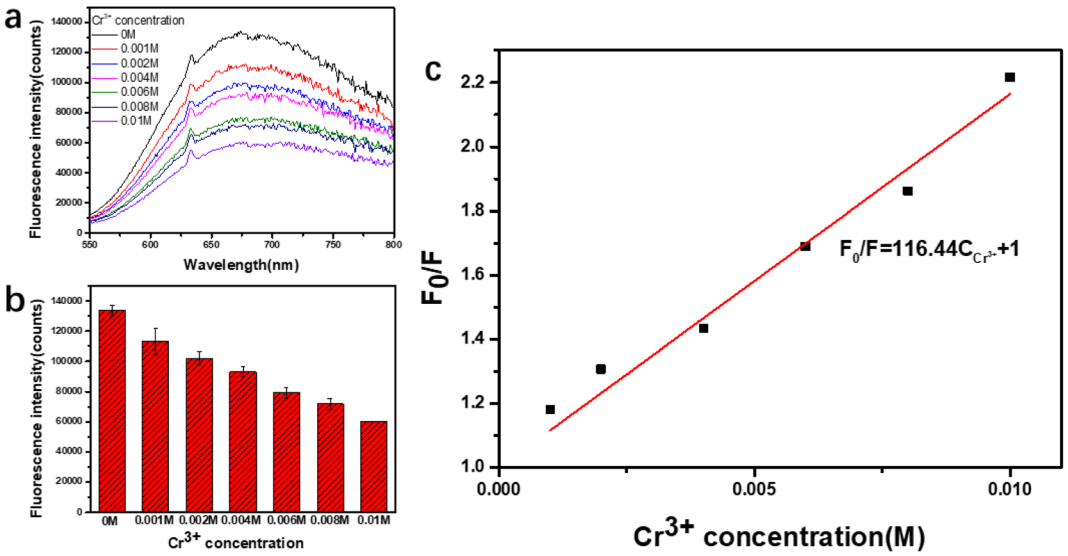

Fig. 6 (a) Fluorescence spectra of PAA–AgNCs with different concentrations of Cr^{3+} ions; (b) the relationship between the fluorescence intensity of PAA–AgNCs and the concentration of Cr^{3+} ions; (c) Stern–Volmer fluorescence quenching curve.

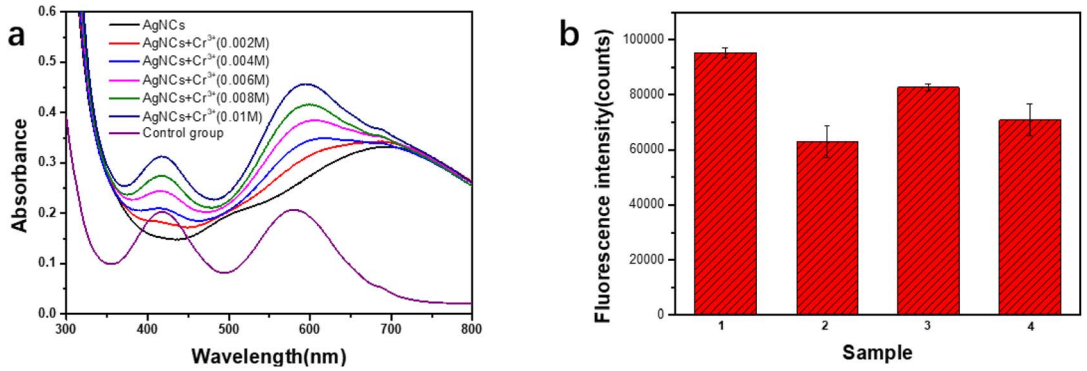

Fig. 7 (a) UV-vis spectra and fluorescence spectra of PAA–AgNCs with different components (control: PAA, isopropanol and Cr^{3+} ions); (b) fluorescence intensity of PAA–AGNCs after Cr^{3+} ions addition under different conditions (1: AgNCs; 2: AgNCs and Cr^{3+} ions; 3: AgNCs, Cr^{3+} ions and PAA (add at the same time); 4: AgNCs, Cr^{3+} ions and PAA (add after fluorescence quenching)).

ions is one of them.[30] Further, according to the UV-vis spectrum (Fig. 7a), with the addition of Cr^{3+} ions, the peak of PAA–AgNCs at 500 nm gradually disappeared, and the peak of PAA–AgNCs at 700 nm began to shift to 580 nm of Cr^{3+} ions, and the characteristic peak at 400 nm of Cr^{3+} ions appeared with the increase of chromium ion concentration, indicating that a new complex without fluorescence emission was formed between Cr^{3+} ions and PAA–AgNCs. Meanwhile, under normal circumstances, the fluorescence intensity of PAA–AgNCs decreases significantly in the presence of Cr^{3+} ions (Fig. 7b). However, when additional PAA exists in the system, part of Cr^{3+} ions was combined with additional PAA without AgNCs binding, the fluorescence intensity of AgNCs will only decrease slightly (Fig. 7b). In addition, after Cr^{3+} ions and PAA–AgNCs were fully combined, and PAA was added into the system. For the addition of new PAA, Cr^{3+} ions and PAA will reach a balance again, so that part of Cr^{3+} ions that has made PAA–AgNCs fluorescence quenched can be separated from PAA–AgNCs. Therefore, the fluorescence intensity of PAA–AGNCs was also slightly increased (Fig. 7b). This also indirectly proved that added Cr^{3+} ions would combine with PAA–AgNCs to form a new complex, resulting in fluorescence static quenching of PAA–AgNCs.

4 Conclusion

In summary, the synthesis of water-soluble fluorescent PAA–AgNCs by irradiation reduction using a simple, inexpensive and commercially available polyelectrolyte PAA as template has proved to be a convenient synthetic method. This fluorescent water-soluble silver nanocluster can control the physical and chemical properties simply by changing the synthesis conditions. The excitation wavelengths and emission wavelengths of the PAA–AgNCs were 517 nm and 679 nm, respectively. Meanwhile, a simple and fast method for Cr^{3+} ions detection was established by using fluorescent PAA–AgNCs as fluorescent probes. In addition, we may expect that this irradiation-reduction method can be extended to the synthesis of other metal nanoclusters.

Author contributions

All authors contributed to the study's conception and design. Data collection was performed by Fei Han and Wenrui Wang. Analysis of data was performed by Fei Han and Jihao Li. The first draft of the manuscript was written by Fei Han under the guidance of Linfan Li. Both authors read and approved the final manuscript.

Conflicts of interest

There is no conflict of interest to declare.

Acknowledgements

This work was supported financially by the Gansu Natural Science Foundation (project no. 20JR10RA778 and no. 20JR10RA777).

References

1 R. Jin, C. Zeng, M. Zhou and Y. Chen, *Chem. Rev.*, 2016, **116**, 10346–10413.
2 L. Shang, S. Dong and G. U. Nienhaus, *Nano Today*, 2011, **6**, 401–418.
3 Y. Lu and W. Chen, *Chem. Soc. Rev.*, 2012, **41**, 3594–3623.
4 Y. Chen, T. Yang, H. Pan, Y. Yuan, L. Chen, M. Liu, K. Zhang, S. Zhang, P. Wu and J. Xu, *J. Am. Chem. Soc.*, 2014, **136**, 1686–1689.
5 I. Diez and R. H. Ras, *Nanoscale*, 2011, **3**, 1963–1970.
6 C. C. Hsu, Y. Y. Chao, S. W. Wang and Y. L. Chen, *Talanta*, 2019, **204**, 484–490.
7 L. Burratti, E. Ciotta, E. Bolli, S. Kaciulis, M. Casalboni, F. De Matteis, A. Garzón-Manjón, C. Scheu, R. Pizzoferrato and P. Prosposito, *Colloids Surf., A*, 2019, **579**, 8.
8 Y. Lu, Y. Mei, M. Schrinner, M. Ballauff, M. W. Moller and J. Breu, *J. Phys. Chem. C*, 2007, **111**, 7676–7681.
9 J. Yu, S. Choi and R. M. Dickson, *Angew. Chem., Int. Ed. Engl.*, 2009, **48**, 318–320.

10 W. Lesniak, A. U. Bielinska, K. Sun, K. W. Janczak, X. Shi, J. R. Baker and L. P. Balogh, *Nano Lett.*, 2005, **5**, 2123–2130.
11 S. Choi, Y. Zhao and J. Yu, *J. Photochem. Photobiol., A*, 2019, **374**, 36–42.
12 L. Shang and S. Dong, *Chem. Commun.*, 2008, 1088–1090, DOI: **10.1039/b717728c**.
13 H. Xu and K. S. Suslick, *ACS Nano*, 2010, **4**, 3209–3214.
14 W. Guo, J. Yuan and E. Wang, *Chem. Commun.*, 2009, 3395–3397, DOI: **10.1039/b821518a**.
15 J. Shen, Z. Wang, D. Sun, G. Liu, S. Yuan, M. Kurmoo and X. Xin, *Nanoscale*, 2017, **9**, 19191–19200.
16 J. Shen, Z. Wang, D. Sun, C. Xia, S. Yuan, P. Sun and X. Xin, *ACS Appl. Mater. Interfaces*, 2018, **10**, 3955–3963.
17 S. M. Ghoreishian, S.-M. Kang, G. S. R. Raju, M. Norouzi, S.-C. Jang, H. J. Yun, S. T. Lim, Y.-K. Han, C. Roh and Y. S. Huh, *Chem. Eng. J.*, 2019, **360**, 1390–1406.
18 S. Singh, A. Guleria, A. K. Singh, M. C. Rath, S. Adhikari and S. K. Sarkar, *J. Colloid Interface Sci.*, 2013, **398**, 112–119.
19 A. Abedini, A. R. Daud, M. A. A. Hamid, N. K. Othman and E. Saion, *Nanoscale Res. Lett.*, 2013, **8**, 10.
20 H. X. Xu and K. S. Suslick, *Adv. Mater.*, 2010, **22**, 1078–1082.
21 L. He, L. F. Dumée, D. Liu, L. Velleman, F. She, C. Banos, J. B. Davies and L. Kong, *RSC Adv.*, 2015, **5**, 10707–10715.
22 Z. Shen, H. Duan and H. Frey, *Adv. Mater.*, 2007, **19**, 349–352.
23 Y. Ding, J. Gao, X. Yang, J. He, Z. Zhou and Y. Hu, *Adv. Powder Technol.*, 2014, **25**, 244–249.
24 L. Shang and S. Dong, *Biosens. Bioelectron.*, 2009, **24**, 1569–1573.
25 R. Konradi and J. r. Ruhe, *Macromolecules*, 2005, **38**, 4345–4354.
26 L. Lu, X. An and W. Huang, *Anal. Methods*, 2017, **9**, 23–27.
27 R. Bencheikh-latmani, A. Obraztsova, M. R. Mackey, M. H. Ellisman and B. M. Tebo, *Environ. Sci. Technol.*, 2007, **41**, 214–220.
28 J. R. Peralta-Videa, M. L. Lopez, M. Narayan, G. Saupe and J. Gardea-Torresdey, *Int. J. Biochem. Cell Biol.*, 2009, **41**, 1665–1677.
29 M. H. Gehlen, *J. Photochem. Photobiol., C*, 2020, **42**, 14.
30 K. Ma, L. Zhao, Z. Jiang, Y. Y. Huang and X. P. Sun, *Polym. Compos.*, 2018, **39**, 1223–1233.